20143B078A

別添１

厚生労働科学研究委託費

革新的がん医療実用化研究事業

（委託業務題目）

「人工核酸YB-1阻害アンチセンス：膵癌に対する新しい分子標的治療の開発」に関する研究

平成２６年度　委託業務成果報告書

業務主任者　中野　賢二

平成２７（２０１５）年 3 月

様式第１８

本報告書は、厚生労働省の科学研究委託事業による委託業務として、国立大学法人九州大学総長　久保 千春（受託者の名称）が実施した平成２６年度「人工核酸YB-1阻害アンチセンス：膵癌に対する新しい分子標的治療の開発」の成果を取りまとめたものです。

別添２

目　　次

別添３

厚生労働科学研究委託費（革新的がん医療実用化研究事業）
委託業務成果報告（総括）

「人工核酸YB-1阻害アンチセンス：膵癌に対する新しい分子標的治療の開発」に関する研究

業務主任者　中野　賢二　九州大学先端融合医療レドックスナビ研究拠点教授

研究要旨

人工核酸YB-1阻害アンチセンスの薬効・薬物動態・安全性の評価を行い、至適投与量・間隔を定める。更に、薬剤の品質及びGMP製造工程を確立し、GLP準拠動物安全性 試験を行って、臨床研究に移行できる基盤を構築する。

中野　賢二・九州大学・教授

Ａ．研究目的

担癌モデルにおける人工核酸YB-1阻害アンチセンスの抗腫瘍効果と安全性の評価を行い、非臨床安全性試験で検討する投与量・間隔を設定することを研究目的とする。加えて、非臨床安全性試験及び研究全体の進捗の統括も行う。

本研究は、橋渡し研究を推進する厚生科学研究行政の有用性を強く社会に発信する。

Ｂ．研究方法

人工核酸YB-1阻害アンチセンスの構造最適化を小比賀らと共同で検討する。人工核酸YB-1阻害アンチセンスの薬効を、担癌マウス血中投与後の腫瘍量をモニターして検討する。腫瘍・正常臓器の組織を採取して免疫染色・ｑRT-PCRにてYB-1発現抑制と血管新生阻害効果を検討する。

安全性に関する検討は斯波らと共同で、放射線・抗癌剤との併用効果は本田らと共同で、膵癌におけるYB-1発現の検討は小田らと共同で実施した（担当者報告書参照）。

（倫理面への配慮）

倫理面での問題は認めない。動物実験は動物実験委員会の承認を得て実施。

Ｃ．研究結果

人工核酸YB-1阻害アンチセンスの配列・構造を最終確定した。

Ｃ．研究結果（続き）

人工核酸YB-1阻害アンチセンス血中投与（10 mg/kg BW）週１回ｘ3回反復投与により膵癌皮下腫瘍モデルにおいて有意な腫瘍の増大抑制効果が認められた。腫瘍組織のYB-1発現抑制がqRT-PCRで確認され、血管新生マーカーCD31染色で評価した微小血管密度はYB-1アンチセンスにより低下した。

安全性、放射線・抗癌剤併用効果、膵癌におけるYB-1発現の検討結果は各担当者の成果報告にまとめた。

Ｄ．考察

安全性に問題ない投与量・間隔の血中投与で、人工核酸YB-1阻害アンチセンスは膵癌に対する抗腫瘍効果を発揮することを担癌マウスモデルで明らかにした。膵癌の対象疾患としての妥当性も確認できた。今後、非臨床安全性試験に向けた投与量を設定する。

Ｅ．結論

人工核酸YB-1阻害アンチセンスは膵癌の分子標的治療薬として有望である。

Ｆ．健康危険情報

健康危害は認めなかった。

Ｇ．研究発表

1. 論文発表：なし
2. 学会発表：なし

Ｈ．知的財産権の出願・登録状況
（予定を含む。）

1. 特許取得
米国仮出願：62/023067（出願日2014.7.10）
Anticancer antisense reagents,
発明人：中野賢二、山本剛史、小比賀聡
2. 実用新案登録：なし
3. その他：なし

別添４

厚生労働科学研究委託費（革新的がん医療実用化研究事業）
委託業務成果報告（業務項目）

「人工核酸YB-1阻害アンチセンスの薬物動態解析法・品質分析法・製造方法の開発支援」に関する研究

担当責任者　小比賀　聡　大阪大学大学院薬学研究科教授

研究要旨

人工核酸YB-1阻害アンチセンスの薬効・薬物動態・安全性の評価を行い、 至適投与量・間隔を定める。更に、薬剤の品質及びGMP製造工程を確立し、GLP準拠動物安全性 試験を行って、臨床研究に移行できる基盤を構築する。

小比賀　聡・大阪大学・教授

Ａ．研究目的

人工核酸YB-1阻害アンチセンスの薬物動態解析の為の技術支援を行い、製剤としての品質分析法、GMP製造方法の開発を検討することを研究目的とする。

Ｂ．研究方法

人工核酸YB-1阻害アンチセンスの構造最適化を中野らと共同で検討する。非臨床安全性試験用人工核酸YB-1阻害アンチセンスの製造方法・品質分析法の開発を製造委託企業に技術支援の形で行う。また、薬物動態解析の為の血中濃度分析法を斯波らと共同で開発する。

（倫理面への配慮）

倫理面での問題は認めない。

Ｃ．研究結果

人工核酸YB-1阻害アンチセンスの配列・構造を最終確定した。血中濃度分析法としてELISA法を確立した。大動物スケールの場合の人工核酸YB-1阻害アンチセンス製造／精製における問題点を検出した。また、品質分析法として、製造原料となる人工核酸アミダイトの各種NMR分析、HPLC解析を実施するとともに、原薬であるアンチセンスおリゴヌクレオチドのHPLC分析およびLC-MASS法の開発を行った。

Ｄ．考察

今回、大量スケールでの人工核酸YB-1阻害アンチセンス製造に適した反応条件を見いだすことができたが、スケールアップに伴い、精製での課題が浮き彫りとなった。今後は、精製ステップにおける純度向上並びに回収量の増加を目指した方法を検討する。

Ｅ．結論

人工核酸YB-1阻害アンチセンスの非臨床安全性試験に向けた製法・品質分析法開発の基盤構築に成功した。

Ｆ．健康危険情報

Ｇ．研究発表

1.　論文発表

T. Yamamoto, A. Yahara, R. Waki, H. Yasuhara, F. Wada, M. H. Shiba, S. Obika: Amido-bridged Nucleic Acids with Small Hydrophobic Residues Enhance Hepatic Tropism of Antisense Oligonucleotides *in vivo*. *Org. Biomol. Chem.*, **2015**, *13*, 3757-3765.

2.　学会発表：なし

（発表誌名巻号・頁・発行年等も記入）

Ｈ．知的財産権の出願・登録状況

（予定を含む。）

1. 特許取得：なし

2. 実用新案登録：なし

3. その他：なし

別添４

厚生労働科学研究委託費（革新的がん医療実用化研究事業）
委託業務成果報告（業務項目）

「人工核酸YB-1阻害アンチセンスの代謝学的な観点からの安全性評価」
に関する研究

担当責任者　斯波　真理子　国立循環器病研究センター内分泌・代謝部長

研究要旨

人工核酸YB-1阻害アンチセンスの薬効・薬物動態・安全性の評価を行い、 至適投与量・間隔を定める。更に、薬剤の品質及びGMP製造工程を確立し、GLP準拠動物安全性 試験を行って、臨床研究に移行できる基盤を構築する。

斯波　真理子・国立循環器病研究センター・部長

Ａ．研究目的

人工核酸YB-1阻害アンチセンスの担癌マウス投与後の代謝・遺伝子変化の観点から安全性評価を行い、至適な投与量、投与間隔等の設定の為の指標を得ることを研究目的とする。

Ｂ．研究方法

人工核酸YB-1阻害アンチセンスの安全性を、血中投与後の体重変化、血液検査、腫瘍以外の正常臓器の所見で、中野らの治療実験のサンプルを用いて評価した。

（倫理面への配慮）

倫理面での問題は認めない。

Ｃ．研究結果

人工核酸YB-1阻害アンチセンス血中投与（10mg/kg BW）週１回ｘ3回反復投与後の体重・血液一般・血液生化学検査に異常を認めなかった。

Ｄ．考察

上記投与量・間隔での人工核酸YB-1アンチセンスの安全性を土台にして、非臨床安全性試験での投与量として、10mg/kg BWを中心とした投与量域を検討する。

Ｅ．結論

治療効果の得られる投与量・投与間隔で、人工核酸YB-1アンチセンスの安全性が確認された。

Ｆ．健康危険情報

Ｇ．研究発表

1.　論文発表

原著論文

1) Yamamoto T, Yahara A, Waki R, Yasuhara H, Wada F, Harada-Shiba M, Obika S: Amido-bridged nucleic acids with small hydrophobic residues enhance hepatic tropism of antisense oligonucleotides *in vivo*. *Organic & Bionolecular Chemistry, in press*

2) Yamamoto T, Fujii N, Yasuhara H, Wada S, Wada F, Shigesada N, Harada-Shiba M, Obika S: Evaluation of multiple-turnover capability of locked nucleic acid antisense oligonucleotides in cell-free rnase h-mediated antisense reaction and in mice. Nucleic acid therapeutics. 24: 283-290, 2014.

総説

1) 小倉正恒, 斯波真理子: 動脈硬化症の治療標的－脂質代謝を中心に, 臨床検査 Vol.59 No.2, 133-141, 2015.2

2) 安原秀典, 和田俊輔, 斯波真理子: 第6節 PCSK9, series モデル動物利用マニュアル 疾患モデルの作製と利用－脂質代謝異常と関連疾患＜上巻＞ 180-194, 2015.1

3) 和田俊輔, 斯波真理子, 小比賀聡: 第５節 ARH, series モデル動物利用マニュアル 疾患モデルの作製と利用－脂質代謝異常と関連疾患＜上巻＞ 169-179, 2015.1

2. 学会発表

（国際学会）

1) Wada S, Saito H, Endo K, Wada F, Yamamoto T, Obika S, Harada-Shiba M, Development of archaeal L7Ae-based siRNA delivery vehicle with apoE mimetic-like effect, 10th Annual Meeting of the Oligonucleotide Therapeutics Society, ポスター発表, 2014 年 10 月 12 日～15 日, San Diego,California, USA

2) Harada-Shiba M, Yamamoto T, Yasuhara H, Wada F, Wada S, Shibata M.A, Obika S, Long Term Effect of Bridged Nucleic Acid(BNA)-Based Antisense Targeting PCSK9 on Metabolism and Inflammation, 82nd European Atherosclerosis Society, ポスター発表, 2014 年 5 月 31 日～6 月 3 日, Madrid Spain

（国内学会）

1) 和田郁人, 山本剛史, 斯波真理子, 小比賀聡, フィブラート系薬剤との比較によるアンチセンス Apolipoprotein C-Ⅲ阻害剤の脂質低下効果の評価, アンチセンス・遺伝子・デリバリーシンポジウム 2014, ポスター発表, 2014 年 9 月 8 日～9 日, 東京

2) 和田俊輔, 石井健, 小比賀聡, 斯波真理子, コレステロール修飾型 siRNA の肝臓における免疫惹起性の増大, アンチセンス・遺伝子・デリバリーシンポジウム 2014, ポスター発表, 2014 年 9 月 8 日～9 日, 東京

3) 山本剛史, 藤井奈緒子, 安原秀典, 斯波真理子, 小比賀聡, アンチセンス核酸の mRNA 切断反応における効率的回転に関する検討, アンチセンス・遺伝子・デリバリーシンポジウム 2014, シンポジウム3, 2014年9月8日～9日, 東京

4) 斯波真理子, 脂質異常症に対するアンチセンス医薬の開発, アンチセンス・遺伝子・デリバリーシンポジウム 2014, シンポジウム 1, 2014 年 9 月 8 日～9 日, 東京

（国内学会：続き）

5) 和田俊輔, 石井健, 小比賀聡, 斯波真理子, コレステロール修飾型 siRNA の肝臓における免疫惹起促進の機序について, 遺伝子・デリバリー研究会 第 14 回夏期セミナー, 2014 年 8 月 20 日～21 日, 一般発表, 熊本

6) 和田郁人, 山本剛史, 小比賀聡, 斯波真理子, コレステロール修飾型アンチセンス核酸の薬理効果及び、体内分布解析, 遺伝子・デリバリー研究会 第 14 回夏期セミナー, 2014 年 8 月 20 日～21 日, 一般発表, 熊本

7) Wada F, Yamamoto T, Obika S, Harada-Shiba M, Effexts of Selective Down-regulation of Apolipoprotein C-Ⅲ by Antisense Oligonucleotides, 第 46 回日本動脈硬化学会総会・学術集会, ポスター発表, 2014 年 7 月 10 日～11 日, 東京

8) Wada S, Yasuhara H, Wada F, Yamamoto T, Obika S, Harada-Shiba M, Conjugation approach toward anti-PCSK9 antisense oligonucleotide agent for getting further inhibitory effedts, 第 46 回日本動脈硬化学会総会・学術集会, ポスター発表, 2014 年 7 月 10 日～11 日, 東京

H. 知的財産権の出願・登録状況
（予定を含む。）

1. 特許取得：なし
2. 実用新案登録：なし
3. その他：なし

別添４

厚生労働科学研究委託費（革新的がん医療実用化研究事業）
委託業務成果報告（業務項目）

「人工核酸YB-1阻害アンチセンスと放射線/ 放射線＋抗癌剤併用効果の検討」に関する研究

担当責任者　本田　浩　九州大学大学院医学研究院臨床放射線学教授

研究要旨

人工核酸YB-1阻害アンチセンスの薬効・薬物動態・安全性の評価を行い、 至適投与量・間隔を定める。更に、薬剤の品質及びGMP製造工程を確立し、GLP準拠動物安全性 試験を行って、臨床研究に移行できる基盤を構築する。

本田　浩・九州大学・教授

Ａ．研究目的

人工核酸YB-1阻害アンチセンスと放射線あるいは放射線・抗癌剤併用による抗腫瘍効果増強の検討を研究目的とする。

Ｂ．研究方法

人工核酸 YB-1 阻害アンチセンスと放射線併用効果の検討: X 線照射と人工核酸 YB-1 アンチセンス、更に抗癌剤および X 線照射・抗癌剤との併用効果を in vitro 培養細胞系において検討する。

（倫理面への配慮）

動物実験は動物実験委員会の承認を得て実施。

Ｃ．研究結果

低濃度YB-1アンチセンス導入により抗癌剤の感受性は2～5倍増加した。また、５Gy2回Ｘ線照射に耐性の膵癌細胞株に低濃度YB-1アンチセンスを導入したところ、殺細胞効果が認められた。

Ｄ．考察

YB-1アンチセンスは放射線・抗癌剤抵抗性を改善する可能性が示唆された。今後、動物実験での併用効果の検討を行う。

Ｅ．結論

人工核酸YB-1阻害アンチセンスと放射線・抗癌剤の併用はより有効性の高い集学的治療法となる可能性が示唆された。

Ｆ．健康危険情報

Ｇ．研究発表

1.　論文発表

Hatakenaka M, Nakamura K, Yabuuchi H, Shioyama Y, Matsuo Y, Kamitani T, Yonezawa M, Yoshiura T, Nakashima T, Mori M, Honda H: Apparent diffusion coefficient is a prognostic factor of head and neck squamous cell carcinoma treated with radiotherapy. Jpn J Radiol 32:80-89. 2014.

2.　学会発表：なし

Ｈ．知的財産権の出願・登録状況
（予定を含む。）

1. 特許取得：なし

2. 実用新案登録：なし

3. その他：なし

別添４

厚生労働科学研究委託費（革新的がん医療実用化研究事業）
委託業務成果報告（業務項目）

「臨床・病理学的解析による膵癌の臨床研究対象としての妥当性の検討と人工核酸YB-1阻害アンチセンスの安全性評価」に関する研究

担当責任者　小田　義直　九州大学大学院医学研究院形態機能病理学教授

研究要旨

人工核酸YB-1阻害アンチセンスの薬効・薬物動態・安全性の評価を行い、 至適投与量・間隔を定める。更に、薬剤の品質及びGMP製造工程を確立し、GLP準拠動物安全性 試験を行って、臨床研究に移行できる基盤を構築する。

小田　義直・九州大学・教授

A．研究目的

患者膵癌のYB-1発現と臨床・病理学的因子との関連を検討し、臨床研究の対象としての膵癌の妥当性に関して検討すること、人工核酸YB-1阻害アンチセンス投与後の担癌マウス正常臓器の組織学的変化を観察し、安全性の検討を行うことを目的とする。

B．研究方法

患者膵癌組織切片を作成し、免疫染色にてYB-1発現を評価し、臨床・病理学的因子との相関を検討した。

（倫理面への配慮）

学内倫理審査会の審査を受け実施。

C．研究結果

YB-1は膵癌症例の82%で高発現し、更にYB-1核内発現は癌にのみ陽性で、分化度・浸潤・予後不良因子との有意な相関が認められた。

D．考察

膵癌においてYB-1は高発現し、悪性化に関与することが明らかとなった。

E．結論

人工核酸YB-1阻害アンチセンス治療薬の臨床研究の対象疾患として膵癌は妥当と考えられる。

F．健康危険情報

G．研究発表

1．論文発表

Mizuuchi Y, Oda Y (10th of 10), et al: Anterior gradient 2 downregulation is mediated by epithelial mesenchymal transition and correlates with poor outcome in pancreatic ductal adenocarcinoma. Lab Invest. 2015; 95(2): 193-206.

Nakata K, Oda Y (5th of 7), et al: Micro RNA-373 is Down-regulated in Pancreatic Cancer and Inhibits Cancer Cell Invasion. Ann Surg Oncol. 2014; 21 Suppl 4: 564-74.

Fujiwara K, Oda Y (10th of 11), et al: CD166/ALCAM Expression Is Characteristic of Tumorigenicity and Invasive and Migratory Activities of Pancreatic Cancer Cells. PLoS One. 2014; 9(9): e107247.

Ideno N, Oda Y (13th of 15), et al: Clinical Significance of GNAS Mutation in Intraductal Papillary Mucinous Neoplasm of the Pancreas With Concomitant Pancreatic Ductal Adenocarcinoma. Pancreas 2015; 44(2): 311-20.

2．学会発表：なし

H．知的財産権の出願・登録状況
（予定を含む。）

1．特許取得：なし

2．実用新案登録：なし

3．その他：なし

様式第１９

学　会　等　発　表　実　績

委託業務題目「人工核酸 YB-1 阻害アンチセンス：膵癌に対する新しい分子標的治療の開発」
機関名 国立大学法人九州大学

１．学会等における口頭・ポスター発表

発表した成果（発表題目、口頭・ポスター発表の別）	発表者氏名	発表した場所（学会等名）	発表した時期	国内・外の別
Development of archaeal L7Ae-based siRNA delivery vehicle with apoE mimetic-like effect. ポスター発表	Wada S, Saito H, Endo K, Wada F, Yamamoto T, Obika S, Harada-Shiba M	San Diego,California, USA (10th Annual Meeting of the Oligonucleotide Therapeutics Society)	2014 年 10 月 12 日～15 日	外国
Long Term Effect of Bridged Nucleic Acid (BNA)-Based Antisense Targeting PCSK9 on Metabolism and Inflammation. ポスター発表	Harada-Shiba M, Yamamoto T, Yasuhara H, Wada F, Wada S, Shibata M.A, Obika S	Madrid, Spain (82nd European Atherosclerosis Society)	2014 年 5 月 31 日～6 月 3 日	外国
フィブラート系薬剤との比較によるアンチセンス Apolipoprotein C-Ⅲ阻害剤の脂質低下効果の評価, ポスター発表	和田郁人, 山本剛史, 斯波真理子, 小比賀聡	東京（アンチセンス・遺伝子・デリバリーシンポジウム 2014）	2014 年 9 月 8 日～9 日	国内
コレステロール修飾型 siRNA の肝臓における免疫惹起性の増大, ポスター発表	和田俊輔, 石井健, 小比賀聡, 斯波真理子	東京（アンチセンス・遺伝子・デリバリーシンポジウム 2014）	2014 年 9 月 8 日～9 日	国内
アンチセンス核酸の mRNA 切断反応における効率的回転に関する検討, シンポジウム	山本剛史, 藤井奈緒子, 安原秀典, 斯波真理子, 小比賀聡	東京（アンチセンス・遺伝子・デリバリーシンポジウム 2014）	2014 年 9 月 8 日～9 日	国内
脂質異常症に対するアンチセンス医薬の開発, シンポジウム	斯波真理子	東京（アンチセンス・遺伝子・デリバリーシンポジウム 2014）	2014 年 9 月 8 日～9 日	国内
コレステロール修飾型 siRNA の肝臓における免疫惹起促進の機序について、 一般発表	和田俊輔, 石井健, 小比賀聡, 斯波真理子	熊本（遺伝子・デリバリー研究会 第 14 回夏期セミナー）	2014 年 8 月 20 日～21 日	国内
コレステロール修飾型アンチセンス核酸の薬理効果及び、体内分布解析、一般発表	和田郁人, 山本剛史, 小比賀聡, 斯波真理子	熊本（遺伝子・デリバリー研究会 第 14 回夏期セミナー）	2014 年 8 月 20 日～21 日	国内
Effexts of Selective Down-regulation of	Wada F, Yamamoto T,	東京（第 46 回日本動脈硬化学会総会・学術集	2014 年 7 月 10 日～11 日	国内

Apolipoprotein C-Ⅲby Antisense Oligonucleotides. ポスター発表	Obika S, Harada-Shiba M	会）		
Conjugation approach toward anti-PCSK9 antisense oligonucleotide agent for getting further inhibitory effedts. ポスター発表	Wada S, Yasuhara H, Wada F, Yamamoto T, Obika S, Harada-Shiba M	東京（第 46 回日本動脈硬化学会総会・学術集会）	2014 年 7 月 10 日～11 日	国内

2．学会誌・雑誌等における論文掲載

掲載した論文（発表題目）	発表者氏名	発表した場所（学会誌・雑誌等名）	発表した時期	国内・外の別
Amido-bridged nucleic acids with small hydrophobic residues enhance hepatic tropism of antisense oligonucleotides *in vivo*.	Yamamoto T, Yahara A, Waki R, Yasuhara H, Wada F, Harada-Shiba M, Obika S	*Organic & Bionolecular Chemistry*	2015	外国
Evaluation of multiple-turnover capability of locked nucleic acid antisense oligonucleotides in cell-free rnase h-mediated antisense reaction and in mice.	Yamamoto T, Fujii N, Yasuhara H, Wada S, Wada F, Shigesada N, Harada-Shiba M, Obika S	Nucleic acid therapeutics	2014	外国
Apparent diffusion coefficient is a prognostic factor of head and neck squamous cell carcinoma treated with radiotherapy.	Hatakenaka M, Nakamura K, YabuuchiH, Shioyama Y, Matsuo Y, Kamitani T, Yonezawa M, Yoshiura T, Nakashima T, Mori M, Honda H	Jpn J Radiol	2014	外国
Anterior gradient 2 downregulation is mediated by epithelial mesenchymal transition and correlates with poor outcome in pancreatic ductal adenocarcinoma.	Mizuuchi Y, Aishima S, Ohuchida K, Shindo K, Fujino M, Hattori M, Miyazaki T, Mizumoto K, Tanaka M, Oda Y	Lab Invest.	2015	外国
Micro RNA-373 is Down-regulated in Pancreatic Cancer and Inhibits Cancer Cell Invasion.	Nakata K, Ohuchida K, Mizumoto K, Aishima S, Oda Y, Nagai E, Tanaka M	Ann Surg Oncol.	2014	外国
Clinical Significance of GNAS Mutation in Intraductal	Ideno N, Ohtsuka T,	Pancreas	2015	外国

Papillary Mucinous Neoplasm of the Pancreas With Concomitant Pancreatic Ductal Adenocarcinoma.	Matsunaga T, Kimura H, Watanabe Y, Tamura K, Aso T, Aishima S, Miyasaka Y, Ohuchida K, Ueda J, Takahata S, Oda Y, Mizumoto K, Tanaka M			
CD166/ALCAM Expression Is Characteristic of Tumorigenicity and Invasive and Migratory Activities of Pancreatic Cancer Cells.	Fujiwara K, Ohuchida K, Sada M, Horioka K, Ulrich CD 3rd, Shindo K, Ohtsuka T, Takahata S, Mizumoto K, Oda Y, Tanaka M	PLoS One	2014	外国

（注１）発表者氏名は、連名による発表の場合には、筆頭者を先頭にして全員を記載すること。

（注２）本様式は excel 形式にて作成し、甲が求める場合は別途電子データを納入すること。

Organic & Biomolecular Chemistry

PAPER

Cite this: *Org. Biomol. Chem.*, 2015, **13**, 3757

Amido-bridged nucleic acids with small hydrophobic residues enhance hepatic tropism of antisense oligonucleotides *in vivo*†

Tsuyoshi Yamamoto,‡[a,b] Aiko Yahara,‡[a] Reiko Waki,[a] Hidenori Yasuhara,[a,b] Fumito Wada,[a,b] Mariko Harada-Shiba[b] and Satoshi Obika*[a]

Received 4th February 2015,
Accepted 5th February 2015

DOI: 10.1039/c5ob00242g

www.rsc.org/obc

High scalability of a novel bicyclic nucleoside building block, amido-bridged nucleic acid (AmNA), to diversify pharmacokinetic properties of therapeutic antisense oligonucleotides is described. *N*2′-functionalization of AmNA with a variety of hydrophobic groups is straightforward. Combinations of these modules display similar antisense knockdown effects and improve cellular uptake, relative to sequence-matched conventional 2′,4′-bridged nucleic acid (2′,4′-BNA) *in vivo*.

Introduction

It has recently been demonstrated that naked therapeutic antisense oligonucleotides (AONs) exhibit robust systemic activity when comprised of several chemically modified nucleic acid building blocks.[1] In particular, conformationally constrained nucleotides such as 2′,4′-bridged nucleic acid (2′,4′-BNA) [also known as locked nucleic acid (LNA)][2] in combination with phosphorothioate (PS) exhibit extraordinarily high target RNA binding and acceptable pharmacokinetics. However, only a small fraction of the administered PS–LNAs is distributed in the target tissues;[3] most of the dose is deposited subcellularly, which is undesirable.[4] Thus, overcoming the pharmacokinetic challenges of AONs is necessary to improve their potency and to address safety concerns.[5]

A number of targeted delivery strategies for antisense therapeutics have been developed, including the terminal conjugation of biofunctional molecules.[6] However, these ligands often interfere with knockdown activity, despite their advantageous effect on the pharmacokinetics of AONs. In contrast, numerous LNA analogues with unique bridging structures have been developed and refined, and apparently minor structural modification of LNA can significantly alter their biological properties.[3a,7] However, the design and synthesis of this class of nucleotides are basically formidable. Therefore, evaluating the pharmacokinetics of AONs is formidable as well because we have only the option of evaluating them *in vivo*. On the other hand, Leumann *et al.* introduced hydrophobic side chains into the C6′-position of each tricyclo-DNA monomer through a metabolically labile ester group, then integrated these nucleotides into oligonucleotides and successfully improved cell-membrane permeability.[8] However, the effect of integration of these monomers on *in vivo* deposition remains obscure. In this context, we recently reported a promising alternative scaffold nucleoside, amido-bridged nucleic acid (AmNA),[9] which may be useful for addressing this issue (Fig. 1).

The furanose of AmNA is fused to a five-membered γ-lactam, whose amide bond is bridged between C2′ and C4′ of the ribose and rigidly fixed in C3′-*endo* conformation. The AmNA-modified AONs are much less susceptible to nuclease digestion than their LNA counterparts, possibly because of the steric hindrance of the *N*2′-methyl and neighboring carbonyl groups of the amide. These modified AONs maintain LNA-like high RNA affinity and show higher *in vitro* antisense activity than their LNA counterparts. Notably, *N*2′-functionalization is usually facile (AmNA[*N*-R]), making AmNA a promising building block for AONs. Other multivalent heteroatom-containing

[a]*Graduate School of Pharmaceutical Sciences, Osaka University, 1-6 Yamadaoka, Suita, Osaka 565-0871, Japan. E-mail: obika@phs.osaka-u.ac.jp; Fax: +81 6 6879 8204; Tel: +81 6 6879 8200*

[b]*Department of Molecular Innovation in Lipidology, National Cerebral and Cardiovascular Center Research Institute, 5-7-1 Fujishirodai, Suita, Osaka 565-8565, Japan*

†Electronic supplementary information (ESI) available. See DOI: 10.1039/c5ob00242g

‡These authors contributed equally to this work.

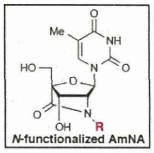

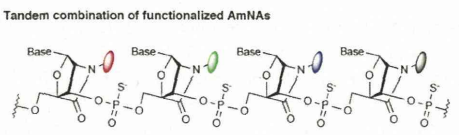

Fig. 1 Tandem arrangement strategy of *N*2′-functionalized AmNAs for improving the pharmacokinetics of antisense therapeutics.

BNAs, such as 2′-amino-LNA,[3c,10] 2′,4′-BNANC,[7f] *N*-Me-aminooxy BNA[7c] and 6′-thiol containing BNA,[11] are also intriguing alternatives in the same context, but *N*- or *S*-functionalized derivatives remain to be comprehensively developed.

To demonstrate the plasticity of our scaffold nucleoside for improving antisense therapeutics, we have developed a methodology to perturb the "*in vivo*" pharmacokinetics of AONs by using a variety of AmNA derivatives. Specifically, we synthesized AmNAs functionalized with a series of hydrophobic groups for potential improvement of intracellular and hepatic uptake of AONs and showed that hydrophobicity of the AmNA-AONs is readily adjustable by altering the substituents. We also demonstrated that a better tandem combination of *N*-alkylated AmNA (AmNA[*N*-R]) modules can improve hepatic disposition and potency of AONs *in vivo*.

Results and discussion

Phosphoramidite monomer synthesis

The phosphoramidite monomers corresponding to AmNA-[*N*-H] **4a** and AmNA[*N*-Me] **4b** were obtained as previously described.[9] From known nucleoside **1**, we synthesized the five monomers AmNA[*N*-Et] **4c**, AmNA[*N*-*n*Pr] **4d**, AmNA[*N*-iPr] **4e**, AmNA[*N*-Bn] **4f** and AmNA[*N*-Phen] **4g**, where abbreviated substituents indicate methyl, ethyl, *n*-propyl, i-propyl, benzyl and phenethyl, respectively (Scheme 1). Briefly, **1** was treated with sodium hydride, followed by the addition of the corresponding alkyl halides to give *N*-substituted compounds **2a–g**. Despite steric hindrance, these coupling reactions provided high yields under optimized conditions. Hydrogenolysis of the *O*3′, *O*5′-benzyl groups as well as *N*3-benzyloxymethyl groups of **2a–g** was effected using palladium on the carbon catalyst in THF followed by *O*5′-dimethoxytritylation to give *N*-substituted monomers **3a–g** in good yield over two steps (52–96%). Subsequent *O*3′-phosphitylation of **3a–g** was achieved with 2-cyanoethyl-*N*,*N*,*N*′,*N*′-tetraisopropylphosphorodiamidite to provide desired thymine phosphoramidites **4a–g**.

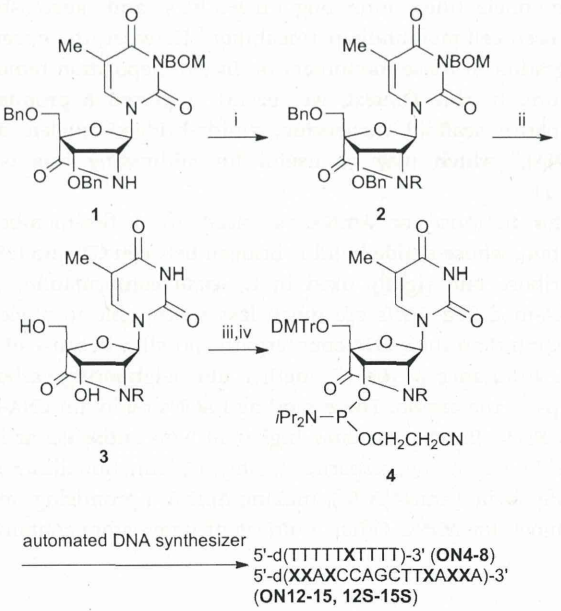

Scheme 1 Reagents and conditions: (i) NaH, RX, DMF, 0 °C → rt, R = Et: EtBr, quant.; R = *n*Pr: *n*PrBr, 76%; R = iPr: iPrI, quant.; R = Bn: BnBr, quant.; R = CH_2CH_2Ph: $BrCH_2CH_2Ph$, 43%; (ii) 20% $Pd(OH)_2/C$, H_2, THF, rt; (iii) DMTrCl, pyridine, rt, R = Et: 74% (2 steps); R = *n*Pr: 96% (2 steps); R = iPr: 81% (2 steps); R = Bn: 90% (2 steps); R = CH_2CH_2Ph: 83% (2 steps); (iv) $(i\text{-}Pr_2N)_2POCH_2CH_2CN$, *N*,*N*-diisopropylammonium tetrazolide, MeCN/THF (3 : 1), rt, R = Et: 77%; R = *n*Pr: 88%; R = iPr: 49%; R = Bn: 61%; R = CH_2CH_2Ph: 48%.

Oligonucleotide synthesis

Synthesis of oligonucleotides (ONs) containing AmNA[*N*-R] monomers was performed on an automated DNA synthesizer using a conventional phosphoramidite method. 5-[3,5-Bis(trifluoromethyl)phenyl]-1*H*-tetrazole (Activator 42®) solution was used for the synthesis of all the oligonucleotides described here. *N*-Alkylated AmNAs **4a–g** were successfully coupled using an extended coupling time to 16 min. The synthesized ONs were purified by reverse-phase HPLC (RP-HPLC) and the composition and purity were analyzed by MALDI-TOF mass spectrometry and RP-HPLC, respectively (Table 1 and ESI Table S1†). A purity greater than 95% was confirmed for all oligonucleotides. Note that the large-scale synthesis of phosphorothioate antisense oligonucleotides for *in vivo* usage and their purification were conducted by Gene Design Inc. (Ibaraki, Japan), where they used AmNA[*N*-R] phosphoramidite monomers provided by us and the composition and purity were analyzed by MALDI-TOF mass spectrometry and RP-HPLC, respectively.

Physicochemical properties of AmNA-containing oligonucleotides

We compared the relative hydrophobicity of oligonucleotides singly modified with AmNAs (**4a–g**; **ON-1–8**) by RP-HPLC using an octadecyl (C18) silica column under the indicated conditions. The obtained retention times are shown in Table 1. AmNA[*N*-H]-modified oligonucleotide **ON-2** was the most

Table 1 Oligonucleotides singly modified with AmNAs[a]

Oligonucleotides	ID	T_m (ΔT_m/mod.) (°C) RNA	DNA	Retention time (min)[b]
5′-d(TTTTTTTTTT)-3′	**ON-1**	19	21	8.4
5′-d(TTTTTt$_H$TTTT)-3′	**ON-2**	26 (+7)	20 (−1)	7.1
5′-d(TTTTTt$_M$TTTT)-3′	**ON-3**	26 (+7)	18 (−3)	10.7
5′-d(TTTTTt$_E$TTTT)-3′	**ON-4**	24 (+5)	18 (−3)	13.5
5′-d(TTTTTt$_n$TTTT)-3′	**ON-5**	21 (+2)	18 (−3)	15.5
5′-d(TTTTTt$_i$TTTT)-3′	**ON-6**	22 (+3)	17 (−4)	17.0
5′-d(TTTTTt$_B$TTTT)-3′	**ON-7**	23 (+4)	18 (−3)	22.4
5′-d(TTTTTt$_P$TTTT)-3′	**ON-8**	21 (+2)	18 (−3)	25.8

[a] t_H = AmNA[*N*-H], t_M = AmNA[*N*-Me], t_E = AmNA[*N*-Et] , t_n = AmNA[*N*-*n*Pr], t_i = AmNA[*N*-iPr], t_B = AmNA[*N*-Bn], and t_P = AmNA[*N*-Phen]. [b] Conditions: eluent A: 0.1 M TEAA buffer, eluent B: A/MeCN (1/1, v/v), gradient: MeCN conc. = 8–13% (30 min), 260 nm.

hydrophilic. As expected, the retention times of the derivatives varied as a function of the hydrophobicity of the oligonucleotides and could be adjusted by changing the substituents and their number.

To estimate the effect of modifications (**4a–g**) on duplex stability, the thermal stability of duplexes was measured with unmodified complementary RNA and DNA strands and compared with the melting temperatures of the corresponding unmodified reference duplexes (Table 1). Single incorporation of AmNAs **4a–g** into the center of a DNA T decamer increased thermal stability for complementary RNA (ΔT_m = +2 to +7 °C), but decreased stability for complementary DNA (ΔT_m = −1 to −4 °C), indicating that high RNA-selective binding is maintained. These results are consistent with previous observations made using a series of BNAs whose bridges differed in size and composition from LNA.[7a,12] A previous crystal structure study of DNA–LNA heteroduplex revealed that the 2′-oxygen of LNA forms hydrogen bonds with water molecules.[13] The perturbation of these hydration patterns by the 2′-substituents of AmNAs probably affected duplex stability, but all derivatives retained high affinity.

Nuclease stability

The effect of AmNA modification on nuclease resistance was determined by incorporating AmNAs into the second base from the 3′-end of oligonucleotides, followed by incubation with CAPV for 40 min at 37 °C. The percentage of intact oligonucleotides was analyzed by RP-HPLC and found to be higher than with conventional AmNA[*N*-Me] (ESI Fig. S5†).[7a]

In vivo activities of AmNA-modified antisense oligonucleotides

We next evaluated hydrophobic AmNA-modified AONs *in vivo*. We previously developed a potent LNA-based AON that targets apolipoprotein CIII (apoC-III) for the treatment of dyslipidemia.[14] Truncated versions of this apoC-III AON were used in these *in vivo* studies because we recently revealed that these could be more potent.[3d,15] Six LNAs were incorporated into a 16-mer PS-AON, **ON-9S**. **ON-10S** retains a seven natural-nucleotide gap moiety, sufficient for maintaining RNase H (a key enzyme for antisense mechanism)-recruiting activity.

The primary purpose of the *in vivo* study was to confirm the effectiveness of this truncated version of LNA-AON to target apoC-III mRNA, and mice were dosed intravenously with **ON-10S** at a dose range of 5–20 mg kg^{-1}. The expression levels of apoC-III mRNA in the liver were analysed 72 hours post-injection. Dose-dependent reduction in hepatic apoC-III mRNA through a single administration of **ON-10S** was observed without significant toxicity (ESI Fig. S6, S7.† The highest reduction in hepatic apoC-III mRNA (60%) was recorded at a dose of 20 mg kg^{-1}, and statistical significance with saline control was found at doses above 10 mg kg^{-1}. Thus, hydrophobic AmNAs-carrying AONs were evaluated *in vivo* at 15 mg kg^{-1}.

N-Alkylated AmNAs **4b, e, f** were introduced into PS-AON **ON-9S** to obtain **ON-11S** to **-13S** as shown in Table 2. The relative hydrophobicity of the oligonucleotides was gauged from their elution time of RP-HPLC.

Table 2 Antisense oligonucleotides targeting murine apoC-III mRNA[a]

Oligonucleotides	ID	T_m (ΔT_m/mod.) (°C) RNA	Retention time (min)[b]
5′-d(TTATCCAGCTTTATTA)-3′	**ON-9S**	39	5.8
5′-d($t_Lt_LAt_LCCAGCTTt_LAt_Lt_LA$)-3′	**ON-10S**	63 (+4)	5.8
5′-d($t_Mt_MAt_MCCAGCTTt_MAt_Mt_MA$)-3′	**ON-11S**	63 (+4)	5.8
5′-d($t_it_iAt_iCCAGCTTt_iAt_it_iA$)-3′	**ON-12S**	61 (+4)	10.6
5′-d($t_Bt_BAt_BCCAGCTTt_BAt_Bt_BA$)-3′	**ON-13S**	59 (+3)	21.2
5′-d($t_it_iAt_MCCAGCTTt_MAt_it_iA$)-3′	**ON-14S**	62 (+4)	11.0
5′-d($t_Bt_MAt_MCCAGCTTt_MAt_Mt_BA$)-3′	**ON-15S**	63 (+4)	13.0

[a] t_L = LNA-T, t_M = AmNA[*N*-Me], t_i = AmNA[*N*-iPr] and t_B = AmNA[*N*-Bn]. [b] Conditions: eluent A: 0.1 M TEAA buffer, eluent B: A/MeCN (1/1, v/v), gradient: MeCN conc. = 13–37% (30 min), 260 nm.

Each PS modification increases the retention time of the AON; consequently the content of acetonitrile in the elution buffer was modified from 8–13% to 13–37%, as described in the footnote to Table 2. The retention times for **ON-11S** to **-13S** differed significantly and predictably from the singly-incorporated phosphodiester-version oligonucleotides (**ON-3, -6, -7**; Table 1). AmNA[*N*-Bn] **4f** and AmNA[*N*-^{i}Pr] **4e** increased the hydrophobicity of the AON, whereas steric hindrance of the gap moiety in **ON-12S** and **-13S** reduced potency. Therefore, we further designed and synthesized **ON-14S** and **-15S**, which showed well-controlled retention times. The T_m values of **ON-11S** to **-15S** were measured and found to be in approximately 60 °C under the indicated buffer conditions. C57Bl/6J male mice (n = 3 per group) were intravenously injected with **ON-10S, -11S, -12S, -13S, -14S** or **-15S** at a dose of 2.9 μmol kg^{-1} (15 mg kg^{-1} for **ON-10S**). LNA counterpart **ON-10S** reduced apoC-III by 45%, and AmNA-AONs **ON-11S** and **ON-12S** achieved a similar knockdown of 40% and 30% respectively. This is the first demonstration of AmNA-AONs exhibiting LNA congener-like high activity *in vivo* (Fig. 2, ESI Fig. S8†). In contrast, AmNA[*N*-Bn] **4f**-based AON **ON-13S** showed no knockdown. The less hindered **ON-14S** and **-15S** in the gaps showed improved potency compared to **-11S, -12S**; interestingly, **ON-14S** achieved the highest knockdown of apoC-III mRNA of the AmNA-AONs tested, suggesting that a combination of functionalized AmNAs working in tandem can tailor potency of AONs.

Hepatic tropism of hydrophobic AmNA-modified antisense oligonucleotides

To investigate whether different combinations of hydrophobic AmNAs alter the tissue deposition of AONs, we measured the intact AONs that accumulated in the liver after intravenous administration using a previously described ELISA method.[16] The hepatic distribution of the more hydrophobic **ON-12S, -13S, -14S** and **-15S** was ~1.5 times higher than that of the LNA-AON **ON-10S**, whereas **ON-10S** and **ON-11S** exhibited

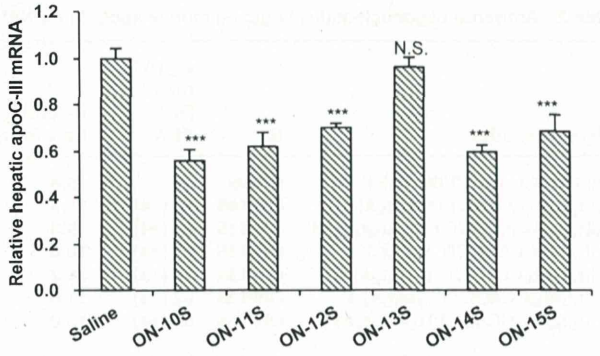

Fig. 2 Reduction of apoC-III mRNA in the livers of mice receiving a single intravenous dose of 2.868 μmol kg^{-1} of a series of AONs. Dunnett's multiple comparison test, ***$P < 0.001$, N.S.; not significant. Error bars represent group means + S.D. $n = 3$.

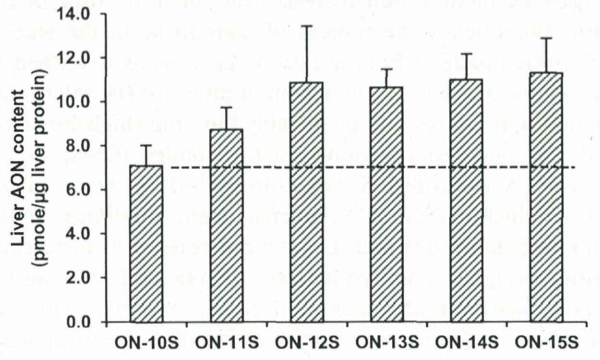

Fig. 3 ELISA-based quantification of a series of AONs distributed in murine liver after 72 hours post-injection. Error bars represent group means + S.D. $n = 3$.

hepatic distribution similar to each other (Fig. 3). However, the activity of all these AmNA-based AONs was at best comparable to the LNA counterpart **ON-10S**. It should primarily be noted that no statistical significance was found between these liver AON contents, which may contribute to this insignificant change in potency. It is also possible that the hydrophobic modification altered the suborgan distribution of AONs in liver. ApoC-III mRNA is predominantly expressed in hepatic parenchymal cells, which comprise 80% of the liver volume, whereas non-parenchymal cells such as Kupffer cells and sinusoidal endothelial cells are relatively minor components of the liver. AONs should therefore selectively target the parenchymal cells. However, it is reported that 80% of PS-AONs accumulated in the liver are distributed in non-parenchymal cells and only 20% are in the parenchymal hepatocytes.[4b] The hydrophobic AONs developed here might foster this trend. Alternatively, there are at least two uptake pathways in parenchymal cells (a productive pathway and a bulk nonproductive pathway); the hydrophobic AONs might encourage the nonproductive uptake which undermines the knockdown activity of AONs.[4a]

Conclusions

In summary, we here showed that AmNAs are an interesting class of antisense building blocks. A series of AmNAs functionalized with a variety of hydrophobic groups were synthesized: AmNA[*N*-Et] **4c**, AmNA[*N*-*n*Pr] **4d**, AmNA[*N*-iPr] **4e**, AmNA-[*N*-Bn] **4f** and AmNA[*N*-Phen] **4g**. We demonstrated that a tandem arrangement of these small substituents affects the systemic activity and tissue disposition of AONs *in vivo*. This strategy will allow more finely-tuned control of the properties of AONs than conventional strategies. Using this scaffold nucleoside, we will further develop useful modules and identify the best combination of these AmNA modules to tackle the issues currently confronting antisense therapeutics.

Experimental

General

All moisture-sensitive reactions were carried out in well-dried glassware under a N_2 atmosphere. Anhydrous dichloromethane, DMF, MeCN, and pyridine were used as purchased. ^{1}H NMR spectra were recorded at 300 and 400 MHz and 500 MHz, ^{13}C NMR were recorded at 75 and 100 MHz, and the ^{31}P spectrum was recorded at 161 MHz. Chemical shift values are expressed in δ values (ppm) relative to tetramethylsilane (TMS) as an internal standard and a residual solvent for ^{1}H NMR, and $CHCl_3$ (δ = 77.00 ppm), methanol (δ = 49.00 ppm), and DMSO (39.50 ppm) for ^{13}C NMR, and 85% H_3PO_4 (δ = 0 ppm) for ^{31}P NMR. Fast atom bombardment mass spectra (FAB-MS) were recorded in the positive ion mode. For column chromatography, silica gel PSQ 100B was used. Progress of the reaction was monitored by analytical thin layer chromatography (TLC) on pre-coated aluminium sheets (Silica gel 60 F_{254} sheet, Merck), and the products were visualized by UV light.

Synthesis of AmNA monomers and phosphoramidites

General procedure 1 (synthesis of compound 2). To the stirring solution of **1** (1.0 equiv.) in DMF (0.1 M) was added NaH (1.2 equiv.) at 0 °C. After stirring for 30 min, alkyl halide (1.2 equiv.) was added. The reaction temperature was gradually raised from 0 °C to room temperature and after completion of the reaction (approx. 30 min), ice-cold water was added. The solution was stirred for 15 min and the product was extracted with ethyl acetate. The organic phase was washed with brine, dried (Na_2SO_4), and concentrated. The product was purified by flash column chromatography (*n*-hexane–ethyl acetate = 3 : 1 or 2 : 1) to afford **2** as a white amorphous solid.

*(2′R)-3′,5′-Di-O-benzyl-N^3-benzyloxymethyl-2′-ethylamino-2′-N,4′-C-oxomethylenethymidine (**2c**: R = Et).* By following the general procedure 1, using bromoethane as an alkyl halide, **2c** was obtained in quant. as a white amorphous solid.

$[\alpha]_D^{23}$ +45.9 (*c* 0.100, $CHCl_3$). IR (KBr): 3071, 3033, 2930, 2871, 1725, 1708, 1665, 1454, 1273 cm^{-1}. ^{1}H NMR (300 MHz, $CDCl_3$) δ: 1.22 (3H, t), 1.64 (3H, s), 3.35 (1H, dq J = 14 Hz,

7 Hz), 3.52 (1H, dq J = 14 Hz, 7 Hz), 3.95, 4.10 (2H, AB, J = 11.5 Hz), 4.07 (1H, s), 4.13 (1H, s), 4.52, 4.54 (2H, AB, J = 12 Hz), 4.59, 4.63 (2H, AB, J = 11.5 Hz), 4.70 (2H, s), 5.39 (1H, s), 5.45, 5.47 (2H, AB, J = 9.5 Hz), 7.18–7.39 (15H, m), 7.54 (1H, s). ^{13}C NMR (100 MHz, $CDCl_3$) δ: 12.8, 13.7, 36.5, 62.4, 63.2, 70.1, 72.2, 72.3, 73.7, 76.7, 78.1, 85.4, 87.6, 109.8, 127.6, 127.6, 127.9, 128.1, 128.4, 133.8, 136.3, 137.4, 137.6, 150.5, 163.1, 170.1. MS (FAB): m/z 612 $[M + H]^+$. HRMS (FAB): calcd for $C_{35}H_{38}N_3O_7$ $[M + H]^+$: 612.2710. Found: 612.2693.

*(2'R)-3',5'-Di-O-benzyl-N^3-benzyloxymethyl-2'-propylamino-2'-N,4'-C-oxomethylenethymidine (**2d**: R = nPr).* By following the general procedure 1, using 1-bromopropane as an alkyl halide, **2d** was obtained in 76% as a white amorphous solid.

$[\alpha]_D^{23}$ +29.2 (c 1.000, $CHCl_3$). IR (KBr): 3066, 3029, 2910, 2863, 1724, 1709, 1664, 1455, 1274 cm^{-1}. ^{1}H NMR (300 MHz, $CDCl_3$) δ: 0.93 (3H, q, J = 7.0 Hz), 1.56–1.64 (2H, m), 1.64 (3H, s), 3.33 (2H, ddq), 3.95, 4.09 (2H, AB, J = 12 Hz), 4.07 (1H, s), 4.13 (1H, s), 4.53 (2H, s), 4.59, 4.65 (2H, AB, J = 11.0 Hz), 4.71 (2H, s), 5.40 (1H, s), 5.46 (2H, t, J = 9.5 Hz), 7.19–7.37 (15H, m), 7.54 (1H, s). ^{13}C NMR (100 MHz, $CDCl_3$) δ: 11.1, 12.9, 21.9, 43.4, 62.9, 63.3, 70.2, 72.3, 72.3, 72.4, 73.8, 78.2, 85.3, 87.5, 109.8, 127.6, 127.6, 127.6, 127.7, 128.0, 128.2, 128.2, 128.2, 128.4, 133.8, 136.3, 137.4, 137.4, 137.7, 150.6, 163.2, 170.5. MS (FAB): m/z 626 $[M + H]^+$. HRMS (FAB): calcd for $C_{36}H_{40}N_3O_7$ $[M + H]^+$: 626.2866. Found: 626.2867.

*(2'R)-3',5'-Di-O-benzyl-N^3-benzyloxymethyl-2'-isopropylamino-2'-N,4'-C-oxomethylenethymidine (**2e**: R = iPr).* By following the general procedure 1, using 2-iodopropane as an alkyl halide, **2e** was obtained in quant. as a white amorphous solid.

$[\alpha]_D^{23}$ +57.2 (c 1.000, $CHCl_3$). IR (KBr): 3064, 3031, 2927, 2873, 1728, 1708, 1666, 1455, 1275 cm^{-1}. ^{1}H NMR (400 MHz, $CDCl_3$) δ: 1.18 (3H, d, J = 7 Hz), 1.31 (3H, d, J = 7 Hz), 1.64 (3H, s), 3.94, 4.10 (2H, AB, J = 12 Hz), 4.07 (1H, s), 4.28 (1H, s), 4.36–4.47 (1H, m), 4.50, 4.54 (2H, AB, J = 11.5 Hz), 4.58, 4.63 (2H, AB, J = 11.5 Hz), 4.71 (2H, s), 5.37 (1H, s), 5.46, 5.49 (2H, AB, J = 9.5 Hz), 7.18–7.39 (15H, m), 7.54 (1H, s). ^{13}C NMR (100.53 MHz, $CDCl_3$) δ: 12.9, 20.6, 21.1, 42.6, 58.9, 63.2, 70.1, 72.2, 72.2, 73.7, 78.2, 86.1, 88.0, 109.6, 127.3, 127.4, 127.5, 127.6, 127.6, 127.9, 128.1, 128.2, 128.2, 128.4, 129.4, 133.8, 136.2, 137.4, 137.7, 150.5, 163.2, 169.4. MS (FAB): m/z 626 $[M + H]^+$. HRMS (FAB): calcd for $C_{36}H_{40}N_3O_7$ $[M + H]^+$: 626.2866. Found: 626.2869.

*(2'R)-3',5'-Di-O-benzyl-N^3-benzyloxymethyl-2'-benzylamino-2'-N,4'-C-oxomethylenethymidine (**2f**: R = Bn).* By following the general procedure 1, using bromomethylbenzene as an alkyl halide, **2f** was obtained in quant. as a white amorphous solid.

$[\alpha]_D^{23}$ +17.1 (c 1.000, $CHCl_3$). IR (KBr): 3064, 3030, 2871, 1728, 1665, 1454, 1277 cm^{-1}. ^{1}H NMR (300 MHz, $CDCl_3$) δ: 1.60 (3H, s), 3.98, 4.12 (2H, AB, J = 12 Hz), 4.20, 4.26 (2H, AB, J = 11 Hz), 4.21, 4.85 (2H, AB, J = 15 Hz), 4.58, 4.65 (2H, AB, J = 11.5 Hz), 4.67 (2H, s), 5.34 (1H, s), 5.39, 5.45 (2H, AB, J = 9.5 Hz), 7.02–7.36 (20H, m), 7.48 (2H, s). ^{13}C NMR (100 MHz, $CDCl_3$) δ: 13.0, 45.1, 61.9, 63.2, 70.3, 72.3, 72.4, 74.0, 77.8, 85.0, 87.5, 109.9, 127.5, 127.7, 127.8, 128.0, 128.1, 128.1, 128.3, 128.4, 128.6, 128.6, 128.8, 133.9, 135.8, 136.2, 137.5, 137.8, 140.0, 150.5, 151.6, 163.3, 170.5. MS (FAB): m/z 674 $[M + H]^+$. HRMS (FAB): calcd for $C_{40}H_{40}N_3O_7$ $[M + H]^+$: 674.2866. Found: 674.2841.

*(2'R)-3',5'-Di-O-benzyl-N^3-benzyloxymethyl-2'-phenethylamino-2'-N,4'-C-oxomethylenethymidine (**2g**: R = CH_2CH_2Ph).* By following the general procedure 1, using 2-bromoethylbenzene as an alkyl halide, **2g** was obtained in 43% as a white amorphous solid.

$[\alpha]_D^{24}$ +0.2 (c 0.320, $CHCl_3$). IR (KBr): 3029, 2930, 1722, 1701, 1667, 1453, 1274 cm^{-1}. ^{1}H NMR (300 MHz, $CDCl_3$) δ: 1.62 (3H, s), 2.82–3.02 (2H, m), 3.52–3.75 (2H, m), 3.94, 4.08 (2H, AB, J = 12 Hz), 4.02 (1H, s), 4.12 (1H, s), 4.44 (2H, s), 4.58, 4.63 (2H, AB, J = 11.5 Hz), 4.70 (2H, s), 5.29 (1H, s), 5.44, 5.48 (2H, AB, J = 9.5 Hz), 7.14–7.40 (20H, m), 7.49 (1H, s). ^{13}C NMR (100.53 MHz, $CDCl_3$) δ: 13.0, 34.7, 43.1, 63.3, 63.3, 70.3, 72.4, 72.5, 74.0, 78.3, 85.3, 87.5, 110.0, 126.7, 127.7, 127.7, 127.8, 128.1, 128.3, 128.3, 128.6, 128.6, 128.7, 133.9, 136.4, 137.5, 137.8, 137.9, 150.6, 163.3, 170.7. MS (FAB): m/z 688 $[M + H]^+$. HRMS (FAB): calcd for $C_{41}H_{42}N_3O_7$ $[M + H]^+$: 688.3023. Found: 688.3015.

General procedure 2 (synthesis of compound 3). To the solution of **2** (1.0 equiv.) in THF or methanol (0.1 M) was added 20% palladium on carbon (1.0 w/w) and the reaction vessel was degassed several times with hydrogen. The reaction mixture was stirred under a hydrogen atmosphere for 1–5 h at room temperature. After completion of the reaction, the reaction solution was filtered using filter paper and washed thoroughly with hot methanol. After evaporation of solvents, the product was dissolved with methanol (0.3 M) and 28% ammonia solution (0.3 M) was added and the solution was stirred at room temperature. After 5 min, the product was concentrated to afford **S1** as a white solid.

To the solution of **S1** in anhydrous pyridine (0.1 M) was added DMTrCl (1.3 equiv.) and the solution was stirred at room temperature. After stirring for 1–19 h, ice-cold water was added and the product was extracted with ethyl acetate. The organic phase was washed with brine, dried (Na_2SO_4), and concentrated. The product was purified by flash column chromatography (n-hexane–ethyl acetate = 1 : 1 or 1 : 3) to afford **3** as a white amorphous solid.

*(2'R)-5'-O-(4,4'-Dimethoxytrityl)-2'-ethylamino-2'-N,4'-C-oxomethylenethymidine (**3c**: R = Et).* By following the general procedure 2, **3c** was obtained in 45% (for 2 steps) as a white amorphous solid.

$[\alpha]_D^{25}$ +12.9 (c 1.000, $CHCl_3$). IR (KBr): 3087, 2967, 2872, 1729, 1698, 1665, 1509, 1464 cm^{-1}. ^{1}H NMR (300 MHz, $CDCl_3$) δ: 1.16 (3H, t, J = 7 Hz), 1.62 (3H, s), 3.23–3.55 (2H, m), 3.63, 3.84 (2H, AB, J = 11.5 Hz), 3.74 (6H, s), 4.10 (1H, s), 4.24 (1H, s), 4.51 (1H, s), 5.39 (1H, s), 6.79–6.83 (4H, m), 7.13–7.45 (9H, m), 7.81 (1H, s), 10.33 (1H, s). ^{13}C NMR (100.53 MHz, $CDCl_3$) δ: 12.4, 13.4, 36.5, 55.1, 56.3, 64.9, 72.6, 85.3, 86.6, 88.8, 110.5, 112.9, 113.2, 127.0, 127.6, 127.8, 127.9, 129.0, 130.0, 135.1, 135.4, 144.3, 150.2, 158.4, 164.6, 170.5. MS (FAB): m/z 636 $[M + Na]^+$. HRMS (FAB): calcd for $C_{34}H_{35}N_3O_8Na$ $[M + Na]^+$: 636.2322. Found: 636.2312.

*(2'R)-5'-O-(4,4'-Dimethoxytrityl)-2'-propylamino-2'-N,4'-C-oxomethylenethymidine (**3d**: R = nPr).* By following the general

procedure 2, **3d** was obtained in 96% (for 2 steps) as a white amorphous solid.

$[\alpha]_D^{26}$ +33.1 (*c* 1.000, $CHCl_3$). IR (KBr): 3384, 3021, 2838, 1704, 1699, 1509, 1254 cm^{-1}. ^1H NMR (300 MHz, $CDCl_3$) δ: 1.17 (3H, t, J = 7 Hz), 1.62 (3H, s), 3.34–3.58 (2H, m), 3.61, 3.90 (2H, AB, J = 12 Hz), 3.91–3.98 (2H, m), 3.88 (6H, s), 4.28 (1H, s), 4.53 (1H, d, J = 7 Hz), 5.50 (1H, s), 6.83–6.85 (4H, m), 7.23–7.36 (7H, m), 7.44 (2H, d, J = 7 Hz), 7.82 (1H, s), 9.40 (1H, s). ^{13}C NMR (75 MHz, $CDCl_3$) δ: 11.2, 12.5, 21.7, 43.6, 55.2, 56.5, 65.2, 72.8, 85.2, 86.9, 88.6, 110.7, 113.3, 113.4, 127.1, 127.9, 128.1, 130.0, 135.1, 135.3, 144.3, 150.1, 158.6, 164.3, 170.6. MS (FAB): *m/z* 650 $[M + Na]^+$. HRMS (FAB): calcd for $C_{35}H_{37}N_3O_8Na$ $[M + Na]^+$: 650.2478. Found: 650.2508.

*(2'R)-5'-O-(4,4'-Dimethoxytrityl)-2'-isopropylamino-2'-N,4'-C-oxomethylenethymidine (**3e**: R = iPr).* By following the general procedure 2, **3e** was obtained in 78% (for 2 steps) as a white amorphous solid.

$[\alpha]_D^{23}$ −3.83 (*c* 1.000, $CHCl_3$). IR (KBr): 3366, 3190, 2968, 2836, 1704, 1686, 1509, 1249 cm^{-1}. ^1H NMR (300 MHz, $CDCl_3$) δ: 1.17 (3H, d, J = 6.5 Hz), 1.28 (3H, d, J = 6.5 Hz), 1.69 (3H, s), 2.54 (1H, s), 3.59, 3.92 (2H, AB, J = 12 Hz), 3.77 (6H, s), 4.28 (1H, s), 4.28–4.37 (1H, m), 4.40 (1H, s), 5.37 (1H, s), 6.82–6.84 (4H, m), 7.20–7.36 (7H, m), 7.44 (2H, d, J = 7 Hz), 7.79 (1H, s), 9.65 (1H, s). ^{13}C NMR (100.53 MHz, $CDCl_3$): δ 12.5, 20.5, 21.1, 42.8, 55.2, 56.5, 61.5, 72.9, 86.0, 86.9, 89.2, 110.6, 113.3, 113.4, 127.1, 127.9, 128.1, 130.0, 135.2, 135.3, 144.4, 150.1, 158.6, 164.3, 169.4. MS (FAB): *m/z* 650 $[M + Na]^+$. HRMS (FAB): calcd for $C_{35}H_{37}N_3O_8Na$ $[M + Na]^+$: 650.2478. Found: 650.2490.

*(2'R)-5'-O-(4,4'-Dimethoxytrityl)-2'-benzylamino-2'-N,4'-C-oxomethylenethymidine (**3f**: R = Bn).* By following the general procedure 2, **3f** was obtained in 90% (for 2 steps) as a white amorphous solid.

$[\alpha]_D^{25}$ +3.8 (*c* 1.000, $CHCl_3$). IR (KBr): 3063, 2967, 2837, 1686, 1607, 1509, 1249 cm^{-1}. ^1H NMR (300 MHz, $CDCl_3$) δ: 1.57 (3H, s), 3.67, 3.88 (2H, AB, J = 12 Hz), 3.74 (6H, s), 4.21 (1H, s), 4.44 (1H, s), 4.47, 4.52 (2H, AB, J = 15 Hz), 5.13 (1H, s), 6.79–6.83 (4H, m), 7.14–7.34 (7H, m), 7.39–7.44 (2H, d, J = 7 Hz), 7.74 (1H, s), 9.97 (1H, s). ^{13}C NMR (75 MHz, $CDCl_3$): δ 12.5, 45.6, 55.2, 56.5, 65.1, 72.4, 84.7, 86.8, 88.7, 110.6, 113.0, 113.3, 127.1, 127.9, 128.0, 128.7, 128.8, 130.0, 135.1, 135.2, 135.7, 144.3, 150.1, 158.6, 164.4, 170.7. MS (FAB): *m/z* 698 $[M + Na]^+$. HRMS (FAB): calcd for $C_{39}H_{37}N_3O_8Na$ $[M + Na]^+$: 698.2478. Found: 698.2484.

*(2'R)-5'-O-(4,4'-Dimethoxytrityl)-2'-phenethyl amino-2'-N,4'-C-oxomethylenethymidine (**3g**: R = CH_2CH_2Ph).* By following the general procedure 2, **3g** was obtained in 84% (for 2 steps) as a white amorphous solid.

$[\alpha]_D^{21}$ +4.6 (*c* 0.400, $CHCl_3$). IR (KBr): 3190, 2958, 2929, 1721, 1694, 1672, 1509, 1270 cm^{-1}. ^1H NMR (300 MHz, $CDCl_3$) δ: 1.67 (3H, d, J = 8.5 Hz), 2.93–3.01 (2H, m), 3.56–3.66 (1H, m), 3.58, 3.87 (2H, AB, J = 12 Hz), 3.81 (7H, m), 4.07 (1H, s), 4.22 (1H, m), 4.34 (1H, s), 5.30 (1H, s), 6.83–7.85 (4H, m), 7.16–7.54 (14H, m), 7.72 (1H, d, J = 8.5 Hz), 8.61 (1H, s). ^{13}C NMR (75 MHz, $CDCl_3$) δ: 13.0, 34.7, 43.1, 63.3, 63.3, 70.3, 72.4, 72.5, 74.0, 78.3, 85.3, 87.5, 109.9, 126.7, 127.7, 127.7, 127.8, 128.1, 128.3, 128.3, 128.6, 128.6, 128.7, 133.9, 136.4, 137.5, 137.8, 137.9, 150.6, 163.3, 170.7. MS (FAB): *m/z* 712 $[M + Na]^+$. HRMS (FAB): calcd for $C_{40}H_{39}N_3O_8Na$ $[M + Na]^+$: 712.2635. Found: 712.2631.

General procedure 3 (synthesis of compound 4). To the solution of **3** (1.0 equiv.) in anhydrous MeCN–THF (3 : 1, 0.1 M) were added *N*,*N*-diisopropylammonium tetrazolide (0.75 equiv.) and 2-cyanoethyl-*N*,*N*,*N*′,*N*′-tetraisopropylphosphorodiamidite (1.2 equiv.). After stirring at room temperature for 9 h–19 h, ice-cold water was added and the product was extracted with ethyl acetate. The organic phase was washed with brine, dried (Na_2SO_4), and concentrated. The product was purified by flash column chromatography (0.05 eq. of triethylamine in *n*-hexane–ethyl acetate = 1 : 1) to afford **4c** (R = Et: 39 mg, 77%) as a white amorphous solid.

*(2'R)-3'-O-[2-Cyanoethoxy(disopropylamino)phosphino]-5'-O-(4,4'-dimethoxytrityl)-2'-ethylamino-2'-N,4'-C-oxomethylenethymidine (**4c**: R = Et).* By following the general procedure 3, **4c** was obtained in 77% as a white amorphous solid.

M.p. 100–103 °C (CH_2Cl_2–hexane). ^{31}P NMR (161.83 MHz, $CDCl_3$) δ: 149.2, 150.3. MS (FAB): *m/z* 814 $[M + H]^+$. HRMS (FAB): calcd for $C_{43}H_{53}N_5O_9P$ $[M + H]^+$: 814.3581. Found: 814.3588.

*(2'R)-3'-O-[2-Cyanoethoxy(disopropylamino)phosphino]-5'-O-(4,4'-dimethoxytrityl)-2'-propylamino-2'-N,4'-C-oxomethylenethymidine (**4d**: R = nPr).* By following the general procedure 3, **4d** was obtained in 88% as a white amorphous solid.

M.p. 83–86 °C (CH_2Cl_2–hexane). ^{31}P NMR (161.83 MHz, $CDCl_3$) δ: 149.8, 150.2. MS (FAB): *m/z* 828 $[M + H]^+$. HRMS (FAB): calcd for $C_{44}H_{55}N_5O_9P$ $[M + H]^+$: 828.3737. Found: 828.3745.

*(2'R)-3'-O-[2-Cyanoethoxy(disopropylamino)phosphino]-5'-O-(4,4'-dimethoxytrityl)-2'-isopropylamino-2'-N,4'-C-oxomethylenethymidine (**4e**: R = iPr).* By following the general procedure 3, **4e** was obtained in 32% as a white amorphous solid.

M.p. 101–104 °C (CH_2Cl_2–hexane). ^{31}P NMR (161.83 MHz, $CDCl_3$) δ: 149.5, 151.3. MS (FAB): *m/z* 828 $[M + H]^+$. HRMS (FAB): calcd for $C_{44}H_{55}N_5O_9P$ $[M + H]^+$: 828.3737. Found: 828.3729.

*(2'R)-3'-O-[2-Cyanoethoxy(disopropylamino)phosphino]-5'-O-(4,4'-dimethoxytrityl)-2'-benzylamino-2'-N,4'-C-oxomethylenethymidine (**4f**: R = Bn).* By following the general procedure 3, **4f** was obtained in 61% as a white amorphous solid.

M.p. 99–101 °C (CH_2Cl_2–hexane). ^{31}P NMR (161.83 MHz, $CDCl_3$) δ: 150.0, 150.2. MS (FAB): *m/z* 876 $[M + H]^+$. HRMS (FAB): calcd for $C_{48}H_{55}N_5O_9P$ $[M + H]^+$: 876.3737. Found: 876.3735.

*(2'R)-3'-O-[2-Cyanoethoxy(disopropylamino)phosphino]-5'-O-(4,4'-dimethoxytrityl)-2'-phenethylamino-2'-N,4'-C-oxomethylenethymidine (**4g**: R = CH_2CH_2Ph).* By following the general procedure 3, **4g** was obtained in 48% as a white amorphous solid.

M.p. 98–101 °C (CH_2Cl_2–hexane). ^{31}P NMR (161.83 MHz, $CDCl_3$) δ: 149.6, 150.8. MS (FAB): *m/z* 890 $[M + H]^+$. HRMS (FAB): calcd for $C_{49}H_{57}N_5O_9P$ $[M + H]^+$: 890.3894. Found: 890.3909.

Synthesis, purification and characterization of oligonucleotides

Synthesis of 0.2 μmol scale of oligonucleotides **ON-6-44** modified with AmNA[*N*-Me] was performed using Oligonucleotide Synthesizer (Gene Design, ns-8) according to the standard phosphoramidite protocol with Activator 42™ (Proligo) as the activator. Dry MeCN was used to dissolve AmNA[*N*-R]. The standard synthesis cycle was used for assembly of the reagents and synthesis of the oligonucleotides, except that the coupling time was extended to 16 minutes for AmNA[*N*-R] monomers. (The coupling time for AmNA[*N*-Me] was 32 seconds.) The synthesis was carried out in trityl on mode and was treated with concentrated ammonium hydroxide at room temperature for 1 h to cleave the synthesized oligonucleotides from the solid support. The oligonucleotides were initially purified by Sep-pack Plus C_{18} Environmental Cartridge. The separated oligonucleotides were further purified by reverse-phase HPLC with Waters Xbridge™ Shield RP_{18} 2.5 μm (10 mm × 50 mm) columns with a linear gradient of MeCN (7–13% over 42 min for **ON-3–6, ON-11, ON-12, ON-16**, 8–15% over 42 min for **ON-7, ON-8**, 13–40% over 42 min for **ON-13, ON-17**) in 0.1 M triethylammonium acetate (pH 7.0). The oligonucleotides were analyzed for purity by HPLC and characterized by MALDI-TOF mass spectroscopy.

UV melting experiments and melting profiles

The UV melting experiments were carried out using a Shimadzu UV-1650 spectrometer equipped with a T_m analysis accessory. Equimolecular amounts of the target RNA or DNA strand and oligonucleotide were dissolved in buffer A (10 mM phosphate buffer at pH 7.2 containing 100 mM NaCl) to give a final strand concentration of 4 μM. The samples were annealed by heating at 95 °C followed by slow cooling to room temperature. The melting profile was recorded at 260 nm from 0 to 70 °C (for **ON-3–8**), from 5 to 100 °C (for **ON-11–13, 16, 17**) at a scan rate of 0.5 °C min^{-1}. The T_m was calculated as the temperature of the half-dissociation of the formed duplexes, determined by the midline of the melting curve.

Enzymatic digestion study

The sample solutions were prepared by dissolving 0.75 μmol of oligonucleotides in 50 mM Tris-HCl buffer (pH 8.0) containing 10 mM $MgCl_2$. To each sample solution, 0.175 μL *Crotalus adamanteus* venom phosphodiesterase (CAVP) was added and the cleavage reaction was carried out at 37 °C. A portion of each reaction mixture was removed at timed intervals and heated to 90 °C for 5 min to deactivate the nuclease. Aliquots of the timed samples were analyzed by RP-HPLC to evaluate the amount of intact oligonucleotides remaining. The percentage of intact oligonucleotide in each sample was calculated and plotted against the digestion time to obtain a degradation curve with time (Fig. S5†).

In vivo knockdown study

All animal procedures were performed in accordance with the guidelines of the Animal Care Ethics Committee of the National Cerebral and Cardiovascular Center Research Institute (Osaka, Japan). All animal studies were approved by an Institutional Review Board. C57BL/6J mice were obtained from CLEA Japan. All mice were male, and studies were initiated when animals were 8 weeks of age. Mice (n = 3 per arm) were maintained on a 12 h light/12 h dark cycle and fed *ad libitum*. Mice were fed a normal chow (CE-2, CLEA Japan) for 2 weeks before and during treatment. Mice received single treatment of saline-formulated AONs intravenously. At the time of sacrifice after 72 hours of injection, mice were subjected to blood collection from tail veins and then anesthetized with isoflurane (Forane, Abbott Japan) under an overnight fasting condition. Livers were harvested and snap frozen until subsequent analysis. Whole blood was collected and subjected to serum separation for subsequent analysis.

mRNA quantification

Frozen liver tissue was collected in a 2 mL tube with 1 mL of TRIzol Reagent (Life Technologies, Japan) and a zirconia ball (⌀ 5 mm, Irie) and mechanically homogenized for 2 min at 30 oscillations per second by a TissueLyser II apparatus (Qiagen). Total RNA was isolated from the resulting suspensions according to the manufacturer's procedure. Gene expression was evaluated by a 2-step quantitative RT-PCR method. Reverse-transcription of RNA samples was performed by using a High Capacity cDNA Reverse-Transcription Kit (Applied Biosystems), and quantitative PCR was performed by TaqMan(R) Fast Universal PCR Master Mix (Applied Biosystems). The mRNA levels of target genes were normalized to the GAPDH mRNA level. For murine apoC-III and GAPDH mRNA quantitation, TaqMan Gene Expression Assay IDs of Mm00445670_m1 and Mm99999915_g1 were used.

ELISA method for AON quantification in liver

Materials and reagents. The template DNA was a 25-mer DNA (5′-gaa tag cga taa taa agc tgg ata a-3′), which is complementary to **ON-9S** to **ON-15S**, with biotin at the 3′-end. The ligation probe DNA was a 9-mer DNA (5′-tcgctattc-3′) with phosphate at the 5′-end and digoxigenin at the 3′-end. The template DNA and the ligation probe DNA were purchased from Japan Bio Service. Reacti-Bind NeutrAvidin-coated polystyrene strip plates were purchased from Thermo Fisher Scientific (Nunc immobilizer streptavidin F96 white, 436015). The template DNA solution (100 nM) was prepared in hybridization buffer containing 60 mM Na_2HPO_4 (pH 7.4), 0.9 M NaCl, and 0.24% Tween 20. The ligation probe DNA solution (200 nM) was prepared in 1.5 units per well of T4 DNA ligase (TaKaRa) with 66 mM Tris-HCl (pH 7.6), 6.6 mM $MgCl_2$, 10 mM DTT and 0.1 mM ATP.

The washing buffer used throughout the assay contained 25 mM Tris-HCl (pH 7.2), 0.15 M NaCl and 0.1% Tween 20. Anti-digoxigenin-AP antibody (Fab fragments conjugated with

alkaline phosphatase) was obtained from Roche Diagnostics. A 1 : 2000 dilution of the antibody with 1 : 10 super block buffer in TBS (Pierce) was used in the assay. The alkaline phosphatase luminous substrate was prepared in 250 μM CDP-Star (Roche) with 100 mM Tris-HCl (pH 7.6) and 100 mM NaCl.

Assay procedures. Frozen liver tissue was collected in a 2 mL tube with 1 mL of PBS and a zirconia ball (Ø 5 mm, Irie) and mechanically homogenized for 2 min at 30 oscillations per second by a TissueLyser II apparatus (Qiagen). Total protein concentrations were measured using a detergent compatible assay kit (Bio-Rad) and adjusted to 8 mg L^{-1} with PBS. The assay was performed at the concentration range of 128 pM to 1000 nM in duplicate. For the standard curve, 7 standard solutions were prepared. To AON-untreated mice liver homogenates were added **ON-10S, ON-11S, ON-12S, ON-13S, ON-14S,** and **ON-15S** solutions to prepare 7 standard samples at a range of 128 pM to 1000 nM. Next, the template DNA solution (100 μL) and standard solution (10 μL) or liver homogenates (10 μL) containing **ON-10S, ON-11S, ON-12S, ON-13S, ON-14S,** and **ON-15S** were added to Reacti-Bind Neutr Avidin-coated polystyrene strip 96-well plates and incubated at 37 °C for 1 h to allow the binding of biotin to streptavidin-coated wells and hybridization. After hybridization, the plate was washed three times with 200 μL of washing buffer. Then, ligation probe DNA solution (100 μL) was added, and the plate was incubated at room temperature (15 °C) for 3 h. The plate was then washed three times with the washing buffer. Subsequently, 200 μL of a 1 : 2000 dilution of anti-digoxigenin-AP was added, and the plate was incubated at 37 °C for 1 h. After washing three times with the washing buffer, the CDP-Star solution was added to the plate, and finally the luminescence intensity was determined by using a Centro XS^3 luminometer (Berthold) one second after the addition of CDP-Star. The linear range of 128 pM to 1000 nM in this ELISA system was determined as $r > 0.97$.

Serum chemistry

Serum from the blood collected from the inferior vena cava upon sacrifice was subjected to serum chemistry. Assay kits (WAKO) were used to measure serum levels of aspartate aminotransferase (AST) and alanine aminotransferase (ALT), which are biomarkers for hepatic toxicity.

Statistics

Statistical comparisons were performed by Dunnett's multiple comparison tests. $^{*}P < 0.05$, $^{**}P < 0.01$, and $^{***}P < 0.001$ were considered to be statistically significant in all cases. N.S. indicates no statistical significance.

Acknowledgements

A part of this work was supported by Basic Science and Platform Technology Program for Innovative Biological Medicine from the Ministry of Education, Culture, Sports, Science and Technology in Japan, JSPS KAKENHI Grant Number 24890102, Grants-in Aid for Scientific Research from the Japanese Ministry of Health, Labor, and Welfare (H23-seisaku tansaku-ippan-004 and H26-kanjitu-kanen-wakate-008) and the Advanced Research for Medical Products Mining Programme from the National Institute of Biomedical Innovation. T.Y. thanks the Grant for Research on Atherosclerosis Update from the Japan Heart Foundation & Astellas/Pfizer. A. Y. thanks the Research Fellowship from the Japan Society for the Promotion of Science (JSPS) for Young Scientists.

Notes and references

1 (*a*) E. R. Rayburn and R. Zhang, *Drug Discovery Today*, 2008, **13**, 513; (*b*) T. Yamamoto, M. Nakatani, K. Narukawa and S. Obika, *Future Med. Chem.*, 2011, **3**, 339.

2 (*a*) S. Obika, D. Nanbu, Y. Hari, K. Morio, Y. In, T. Ishida and T. Imanishi, *Tetrahedron Lett.*, 1997, **38**, 8735; (*b*) S. K. Singh and J. Wengel, *Chem. Commun.*, 1998, 1247.

3 (*a*) T. Yamamoto, M. Harada-Shiba, M. Nakatani, S. Wada, H. Yasuhara, K. Narukawa, K. Sasaki, M. A. Shibata, H. Torigoe, T. Yamaoka, T. Imanishi and S. Obika, *Mol. Ther. Nucleic acids*, 2012, **1**, e22; (*b*) K. Fluiter, A. L. ten Asbroek, M. B. de Wissel, M. E. Jakobs, M. Wissenbach, H. Olsson, O. Olsen, H. Oerum and F. Baas, *Nucleic Acids Res.*, 2003, **31**, 953; (*c*) K. Fluiter, M. Frieden, J. Vreijling, C. Rosenbohm, M. B. De Wissel, S. M. Christensen, T. Koch, H. Orum and F. Baas, *ChemBioChem*, 2005, **6**, 1104; (*d*) E. M. Straarup, N. Fisker, M. Hedtjarn, M. W. Lindholm, C. Rosenbohm, V. Aarup, H. F. Hansen, H. Orum, J. B. Hansen and T. Koch, *Nucleic Acids Res.*, 2010, **38**, 7100.

4 (*a*) R. S. Geary, E. Wancewicz, J. Matson, M. Pearce, A. Siwkowski, E. Swayze and F. Bennett, *Biochem. Pharmacol.*, 2009, **78**, 284; (*b*) M. J. Graham, S. T. Crooke, D. K. Monteith, S. R. Cooper, K. M. Lemonidis, K. K. Stecker, M. J. Martin and R. M. Crooke, *J. Pharmacol. Exp. Ther.*, 1998, **286**, 447.

5 (*a*) E. E. Swayze, A. M. Siwkowski, E. V. Wancewicz, M. T. Migawa, T. K. Wyrzykiewicz, G. Hung, B. P. Monia and C. F. Bennett, *Nucleic Acids Res.*, 2007, **35**, 687; (*b*) E. P. van Poelgeest, R. M. Swart, M. G. Betjes, M. Moerland, J. J. Weening, Y. Tessier, M. R. Hodges, A. A. Levin and J. Burggraaf, *Am. J. Kidney Dis.*, 2013, **62**, 796.

6 (*a*) O. Nakagawa, X. Ming, L. Huang and R. L. Juliano, *J. Am. Chem. Soc.*, 2010, **132**, 8848; (*b*) T. P. Prakash, M. J. Graham, J. H. Yu, R. Carty, A. Low, A. Chappell, K. Schmidt, C. G. Zhao, M. Aghajan, H. F. Murray, S. Riney, S. L. Booten, S. F. Murray, H. Gaus, J. Crosby, W. F. Lima, S. L. Guo, B. P. Monia, E. E. Swayze and P. P. Seth, *Nucleic Acids Res.*, 2014, **42**, 8796; (*c*) J. Winkler, *Ther. Delivery*, 2013, **4**, 791.

7 (*a*) S. M. A. Rahman, S. Seki, S. Obika, H. Yoshikawa, K. Miyashita and T. Imanishi, *J. Am. Chem. Soc.*, 2008, **130**, 4886; (*b*) P. P. Seth, A. Siwkowski, C. R. Allerson,

